Research Square

Preprints are preliminary reports that have not undergone peer review.
They should not be considered conclusive, used to inform clinical practice,
or referenced by the media as validated information.

Engineering Detachable Hyaluronic Acid Microneedles for Controlled Intradermal Delivery of Particulate and Molecular Colorants: Influence of Matrix Cross-Linking and Particle Size

Kornkamol Obthong
Chulalongkorn University
Supanan Ampawa
Mineed Technology
Supason Wanichwecharungruang
supason.p@chula.ac.th

Chulalongkorn University

Research Article

Keywords: Detachable microneedles, Tattoo pigments, FD&C dyes, Natural dyes, Pigment particle size, Colorant diffusion, Hyaluronic acid, Cross-linked hydrogel

Posted Date: February 26th, 2026

DOI: https://doi.org/10.21203/rs.3.rs-8899289/v1

License: This work is licensed under a Creative Commons Attribution 4.0 International License.
Read Full License

Additional Declarations: No competing interests reported.

Abstract

Controlled intradermal placement of colorants remains a challenge in materials research due to the competing effects of molecular solubility, particle size, and matrix interactions on retention and diffusion, with implications for medical reconstructive marking and aesthetic applications. In this study, we evaluate a detachable hyaluronic acid (HA) microneedle platform as a delivery system for depositing a diverse set of colorants spanning multiple chemical classes. Microneedle patches were fabricated from HA and loaded with fifteen colorants, including conventional synthetic pigments, Food, Drug, and Cosmetic (FD&C) dyes, natural pigments, and natural dyes. All formulations demonstrated sufficient mechanical strength (withstanding up to 70 N) to enable reliable insertion into *ex vivo* porcine skin and reproducible transfer of colorant-loaded needles. Comparative assessment revealed that conventional synthetic pigments produced the most vivid and spatially stable intradermal patterns, whereas molecular dyes exhibited broader diffusion and reduced pattern persistence. Pigment particle size emerged as a key determinant of local retention: intermediate-sized particles (3–5 μm) yielded sharper and more persistent patterns than smaller particulates. Furthermore, increasing the cross-linking density of the HA matrix effectively restricted the diffusion of hydrophobic dyes, providing a materials-based strategy for tuning the spatial precision of intradermal deposits. These findings establish a rational design framework for tailoring intradermal delivery systems to meet specific requirements for precision, duration, and visual outcome in dermatological and reconstructive procedures.

1. Introduction

Intradermal pigmentation is a critical technique utilized in both medical and aesthetic dermatology. Beyond its common use in decorative tattooing, the precise placement of colorants within the skin is essential for reconstructive procedures, including repigmentation of vitiligo-affected tissue, areola reconstruction following mastectomy, and permanent marking for radiotherapy target localization [1–3]. Despite its widespread application, conventional intradermal delivery relies primarily on manual needles or mechanical tattoo machines. These approaches frequently result in permanent coloration, significant epidermal trauma, and potential complications, including localized infection and inflammatory reactions to synthetic pigments [4, 5].

Recent advances in materials science have introduced microneedle-based platforms as alternative approaches for intradermal delivery. Dissolvable microneedle tattoo patches have been reported as single-use systems capable of delivering various cargoes, including colorants, into the skin [6]. While these systems enhance reproducibility and user convenience, incomplete needle dissolution and inconsistent pattern transfer remain important limitations. Prolonged application times and sustained pressure are often required to ensure complete needle separation, and partial needle retention in the backing layer can result in incomplete pattern transfer.

Beyond delivery mechanics, the physicochemical properties of colorants critically influence diffusion, retention, and pattern stability following intradermal deposition. Tattoo-related adverse reactions are

frequently associated with immunological responses to pigments and their degradation products [1, 7–9]. Many synthetic tattoo pigments are composed of polycyclic, phthalocyanine, or azo-based structures and may contain trace heavy metals, raising concerns regarding long-term dermal accumulation and chemical safety [10, 11]. Migration of pigment particles from the dermal deposition site to regional lymph nodes has been demonstrated, with particle size and chemical composition identified as key determinants of this behavior [9, 12, 13]. In 2022, the European Union implemented new restrictions under the Registration, Evaluation, Authorisation and Restriction of Chemicals (REACH) Regulation, prohibiting tattoo inks from containing substances considered harmful to human health. Nevertheless, concerns regarding ink composition, degradation products, and regulatory compliance continue to be reported [14].

From a materials perspective, tattoo persistence reflects a balance between colorant immobilization and diffusion. Insoluble pigment particles generally remain localized within the skin, whereas molecular dyes, due to their small size and high solubility, diffuse more rapidly and fade faster. Despite this distinction, systematic comparisons of pigments and dyes with different chemical classes and particle sizes in tattoo applications remain limited. Reports on the use of Food, Drug, and Cosmetic (FD&C) dyes and natural colorants are particularly scarce [15]. These materials typically exhibit high water solubility and reduced chemical stability, resulting in temporary or short-lived tattoo patterns, as exemplified by natural dyes such as henna or jagua [16].

While microneedles have been extensively studied for the delivery of small molecules and vaccines, their application as precision tools for colorant deposition remains underexplored [6, 15]. In particular, the effects of microneedle matrix cross-linking density, colorant solubility, and pigment particle size on the resulting visual and spatial outcomes have not been systematically investigated. Understanding these parameters is essential for engineering devices capable of producing either sharp, high-definition lines for reconstructive marking or soft, diffused gradients for aesthetic applications such as cheek or lip tinting. Furthermore, such understanding may enable the more effective use of biocompatible natural colorants, including those with anti-inflammatory and antioxidant properties [17].

In this work, we systematically investigate a detachable hyaluronic acid (HA) microneedle platform for the delivery of fifteen chemically distinct colorants, including synthetic pigments, FD&C dyes, and natural alternatives. We evaluate how colorant chemical class, pigment particle size, and HA matrix cross-linking density collectively influence deposition efficiency and spatial retention in *ex vivo* porcine skin. By characterizing the skin patterning across various colorant classes and probing the influence of HA cross-linking on lateral diffusion, this work establishes the fundamental design principles required to optimize microneedle systems for clinical and aesthetic applications.

2. Materials and Methods

2.1 Materials

HA with molecular weights of 2000 kDa (high-Mw-HA) and 5 kDa (low-Mw-HA), as well as sorbitol, were purchased from Baoding Faithful Industry Co., Ltd. (Baoding, Hebei, China). 1,4-Butanediol diglycidyl ether (BDDE) was obtained from Tokyo Chemical Industry Co., Ltd. (Tokyo, Japan). Sodium hydroxide was purchased from Merck (Darmstadt, Germany). Lint-free polyester sheets (gamma-sterilized prior to use) were supplied by Mineed Technology (Bangkok, Thailand). Dry powdered tattoo pigments, including a phthalocyanine-based blue tattoo pigment (hereafter referred to as blue tattoo pigment; Navy Blue, TN15, Lot No. 210903), an azo-based yellow tattoo pigment (hereafter referred to as yellow tattoo pigment; Mellow Yellow, TN13, Lot No. 907160), and an azo-based red tattoo pigment (hereafter referred to as red tattoo pigment; Horizon Red, TN50, Lot No. 216150), were obtained from National Tattoo Supply (Allentown, PA, USA). Additional powdered pigments, including carbon black, melanin black, bamboo charcoal (particle sizes of 1–2 μm, 3–5 μm, 4–9 μm, and 0.3–0.7 mm), and beta-carotene, as well as powdered natural dyes (butterfly pea, gardenia blue, curcumin, beetroot, and red yeast rice) and Food, Drug, and Cosmetic (FD&C) dyes (FD&C Blue No. 1, Yellow No. 5, and Red No. 40), were purchased from Chanjao Longevity Co., Ltd. (Bangkok, Thailand). Carbopol, 1,2-hexanediol, and caprylyl glycol were obtained from the same supplier. Sucrose was purchased from Lab Valley Ltd., Part. (Bangkok, Thailand). Ethanol was obtained from RCI Labscan Co., Ltd. (Bangkok, Thailand). Sodium benzoate and potassium sorbate were purchased from Chemipan Corporation Co., Ltd. (Bangkok, Thailand), and citric acid was obtained from Carlo Erba Reagents (Rodano, Milan, Italy).

Silicone microneedle molds containing forty-six conical cavities (depth: 1.06 mm, base diameter: 0.40 mm), arranged in a heart-shaped pattern with a center-to-center needle spacing of 0.55 mm (Fig. S1 in the Supplementary Information, SI), were obtained from Mineed Technology (Bangkok, Thailand). Fresh porcine ear skin from crossbred pigs (*Sus scrofa domesticus*) was obtained from a local slaughterhouse and transported under cold-chain conditions (4°C) prior to use.

2.2 Fabrication of Detachable Dissolvable Microneedle Tattoo Patches

Detachable dissolvable microneedle tattoo patches were fabricated using a two-step mold-casting procedure. The microneedle (needle) layer was first formed by casting a colorant-containing HA solution into the mold cavities, followed by formation of the base layer using a separate casting solution after drying of the needle layer.

2.2.1 Preparation of needle-layer casting solution

Two HA-based needle matrices were prepared: non-cross-linked HA and cross-linked HA (cHA).

For non-cross-linked HA microneedles, a 3% (w/v) HA stock solution was prepared by dissolving high-Mw-HA in distilled water. The solution was autoclaved at 121°C for 15 min, cooled to room temperature, and stored at 4°C until use (pH ≈ 5).

Pigment-type colorants (blue tattoo pigment, yellow tattoo pigment, red tattoo pigment, carbon black, melanin black, bamboo charcoal, and beta-carotene) were dispersed in 1% (w/v) sucrose in ethanol to a final concentration of 0.5% (w/v). Curcumin was dissolved in the same solvent system at an equivalent concentration. Dye-type colorants (butterfly pea, gardenia blue, beetroot, red yeast rice, and FD&C dyes) were dissolved in 1% (w/v) sucrose aqueous solution at 0.5% (w/v). Each colorant suspension or solution was then mixed with the HA stock solution at a volume ratio of 1:1 to obtain the final needle-layer casting solution.

cHA was prepared following a previously reported method [18]. Briefly, an 8% (w/v) HA solution was prepared in 0.25 mM NaOH, autoclaved at 121°C for 15 min, cooled, and reacted with 0.0028% BDDE (weight BDDE/weight HA). The reaction mixture was incubated at 40°C for 72 h. The resulting cHA gel (pH ≈ 8) was stored at 4°C until use. Selected colorants (curcumin, gardenia blue, and FD&C dyes) were mixed with the cHA gel at a 1:1 (v/v) ratio prior to casting.

2.2.2 Preparation of base-layer casting solution

The base-layer casting solution consisted of low-Mw-HA (8% w/v), sorbitol (1.5% w/v), carbopol (0.4% w/v), 1,2-hexanediol (0.05% w/v), and caprylyl glycol (0.05% w/v) dissolved in distilled water.

2.2.3 Mold casting procedure

Microneedle patches were fabricated using a two-step mold-casting process under reduced pressure. First, 300 µL of the needle-layer casting solution was dispensed into the mold cavities under vacuum and allowed to air-dry. Subsequently, 100 µL of the base-layer casting solution was applied over the dried needle layer and air-dried. A polyester backing sheet was then laminated onto the base layer using a fine water mist to promote adhesion. The finished microneedle patches were stored in airtight containers until use.

For solubility testing, microneedles were fabricated using only the needle-layer casting solution, without the base layer or backing sheet.

2.3 Mechanical Characterization

Mechanical properties of the microneedle patches were evaluated using a universal testing machine (UTM) (Shimadzu EZ-S, Shimadzu Corp., Tokyo, Japan). Each patch was placed needle-side up on a glass slide mounted on the stationary plate. A flat compression probe (2 cm in diameter) was advanced toward the sample at a rate of 1 mm min^{-1}, with a maximum applied force of 200 N. Force–displacement curves were recorded, and measurements were performed in triplicate. Microneedle morphology before and after compression was examined using a stereomicroscope (Olympus JP22, Japan).

2.4 Dissolution and Swelling of Cross-Linked HA Microneedles

The dissolution and swelling behavior of cHA microneedles were evaluated as previously described [18]. Five cHA microneedle samples were immersed in 20 mL of distilled water for 30 min, removed using a sieve, and allowed to drain. The swollen samples were weighed and subsequently dried at 50°C for 3 days prior to reweighing. Swelling ratios were calculated relative to the dry mass.

2.5 Administration to *Ex Vivo* Porcine Skin

Fresh porcine ear skin was rinsed with distilled water, shaved, and gently dried. Microneedle patches were manually pressed onto the skin for 10 s, followed by application of three drops of distilled water onto the polyester backing. The patch was then pressed for an additional 1 min before removal. The skin surface was immediately examined using a stereomicroscope.

2.6 Needle Embedment and Colorant Diffusion Analysis

To evaluate needle embedment, tattooed skin samples were cross-sectioned immediately after patch removal along the tattoo pattern and examined under a stereomicroscope. Penetration depth was measured as the distance from the stratum corneum surface to the distal end of the visible color region.

For diffusion studies, tattooed skin samples were placed in closed Petri dishes containing preservative-soaked paper towels and stored at 4°C. Observations were performed at 0, 1, 3, and 5 h, and 7 days after application. Diffusion was qualitatively assessed from stereomicroscopic images of both surface and cross-sectioned samples and quantitatively estimated using the ratio of color intensity measured at depths of 0.3 mm and 0.05 mm from the stratum corneum.

2.7 Statistical Analysis

Data are presented as mean ± standard deviation (SD). Statistical analysis was performed using one-way analysis of variance (ANOVA) followed by Tukey's post-hoc test (GraphPad Prism 10, GraphPad Software Inc., San Diego, CA, USA). Differences were considered statistically significant at $p < 0.05$.

3. Results and Discussion

3.1 Morphology and Mechanical Properties of Tattoo Microneedle Patches

Stereomicroscopic images confirmed that all tattoo microneedle patches consisted of forty-six conical microneedles arranged in a heart-shaped pattern (Fig. 1A–O), with overall dimensions consistent with those of the silicone mold (Fig. S1C and D in the SI). Individual microneedles exhibited a uniform conical geometry with an average height of approximately 1000 μm and a base diameter of 400 μm. No visible defects, incomplete filling, or structural collapse were observed across patches loaded with different colorants, indicating that incorporation of pigments or dyes did not adversely affect microneedle formation.

Mechanical characterization showed that all microneedle patches withstood compressive forces in the range of 55–70 N, with needle displacement values of 0.005–0.01 mm N^{-1}. These values are comparable to or exceed those reported for dissolvable microneedle systems capable of consistent skin insertion [19, 20]. Minor variations in force–displacement behavior were observed among formulations containing different colorants; however, all patches retained sufficient mechanical integrity to maintain needle shape during compression. The favorable mechanical performance is attributed primarily to the use of high-Mw-HA (2000 kDa) as the structural matrix, supplemented by sucrose to enhance stiffness and reduce shrinkage during drying.

Collectively, these results demonstrate that a broad range of pigments and dyes can be incorporated into HA microneedles without compromising structural robustness.

3.2 Transfer of Tattoo Patterns onto *Ex Vivo* Porcine Skin

All fifteen microneedle formulations successfully transferred their predefined heart-shaped patterns onto *ex vivo* porcine skin following application (Fig. 2). Visual inspection of the polyester backing sheets after patch removal revealed no residual needles or fragments (representative examples shown in Fig. 3), confirming complete detachment and reliable intradermal deposition of the microneedles. This consistent needle transfer highlights a key advantage of the detachable microneedle design over conventional dissolvable microneedles, where incomplete needle separation can result in pattern loss.

Despite comparable microneedle morphology, the clarity and intensity of the transferred tattoo patterns varied substantially depending on the type of colorant incorporated. Among black colorants, microneedles loaded with carbon black and bamboo charcoal produced darker and more clearly defined patterns than those containing melanin black (Fig. 2A–C). Cross-sectional analysis confirmed successful intradermal deposition of all three black colorants; however, the color intensity of melanin black within the tissue was markedly lower. This reduced visibility is likely attributable to the poorer dispersibility and lower effective color strength of melanin black under the formulation conditions used.

Among the remaining colorants, vivid and well-defined patterns were obtained from microneedles loaded with commercial tattoo pigments (blue tattoo pigment, yellow tattoo pigment, and red tattoo pigment), FD&C dyes (FD&C Blue No. 1, Yellow No. 5, and Red No. 40), and selected natural dyes (gardenia blue, curcumin, and red yeast rice) (Fig. 2D–I, K, M, and O). In contrast, microneedles containing butterfly pea, beetroot, or beta-carotene produced faint or poorly discernible patterns (Fig. 2J, L, and N). Cross-sectional images showed that these latter colorants exhibited minimal visible deposition within the skin, consistent with their lower intrinsic color intensity at the tested loading levels.

Based on pattern clarity and intradermal visibility, twelve colorants were selected for further diffusion and retention analysis, whereas formulations yielding faint patterns (butterfly pea, beetroot, or beta-carotene) were excluded from subsequent evaluation.

3.3 Diffusion Behavior and Pattern Stability

The temporal stability of tattoo patterns was assessed by monitoring both skin surface appearance and intradermal color distribution over a seven-day period. Skin samples were maintained under hydrated conditions at 4°C to minimize dehydration effects.

Tattoo patterns generated from carbon black showed minimal lateral or vertical diffusion throughout the observation period, retaining sharp boundaries and high contrast (Fig. 2A and a). Bamboo charcoal exhibited slightly greater diffusion, accompanied by gradual fading (Fig. 2B and b), while melanin black produced weak and diffuse patterns from the outset (Fig. 2C and c). These observations are consistent with previous reports describing the high stability of carbon black-based tattoo pigments [21].

The three commercial tattoo pigments (blue tattoo pigment, yellow tattoo pigment, and red tattoo pigment) displayed excellent spatial stability, with negligible diffusion and only minor intensity loss over time (Fig. 2D–F and d–f). In contrast, FD&C dyes (FD&C Blue No. 1, Yellow No. 5, and Red No. 40) exhibited pronounced diffusion, manifested as lateral spreading and deeper penetration into the tissue over time (Fig. 2G–I and g–i). Similar diffusion behavior was observed for curcumin and red yeast rice, whereas gardenia blue displayed the most rapid diffusion and pronounced fading (Fig. 2K, M, O and k, m, o).

These results clearly distinguish pigment-type colorants from dye-type colorants in terms of intradermal mobility. Pigments, which exist as insoluble particulate matter, remain relatively localized following deposition, whereas molecular dyes readily diffuse through the hydrated tissue environment. This behavior reflects fundamental differences in particle size, solubility, and interactions with the surrounding matrix.

3.4 Effect of Pigment Particle Size on Diffusion

To further elucidate the role of particle size, bamboo charcoal pigments with four different size ranges (1–2 μm, 3–5 μm, 4–9 μm, and 0.3–0.7 mm) were incorporated into microneedles and evaluated. Pigments with particle sizes of 1–2 μm, 3–5 μm, and 4–9 μm were successfully cast into microneedles, producing uniform needle loading. In contrast, the largest particles (0.3–0.7 mm) could not be effectively incorporated into the microneedle cavities, resulting in poor pattern transfer (Fig. 4).

Among the successfully fabricated formulations, bamboo charcoal particles in the 3–5 μm range produced the darkest and most persistent tattoo patterns, outperforming both smaller and larger particles (Fig. 4). These findings indicate that particle size influences not only the manufacturability of pigment-loaded microneedles but also the quality and durability of the resulting tattoo patterns. Intermediate particle sizes appear to provide an optimal balance between color intensity, dispersion within the microneedle matrix, and retention within the skin.

3.5 Influence of HA Cross-Linking on Dye Diffusion

The effect of matrix structure on dye diffusion was examined by comparing microneedles fabricated from non-cross-linked HA and cHA. Unloaded cHA microneedles exhibited swelling without complete

dissolution when immersed in water, whereas non-cross-linked HA microneedles dissolved completely within 30 min, confirming successful cross-linking of the HA network.

Microneedles loaded with curcumin (hydrophobic natural dye), gardenia blue (water-soluble natural dye), and FD&C Blue No. 1 (water-soluble synthetic dye) were evaluated to assess the influence of cross-linking on diffusion behavior. cHA significantly reduced the diffusion of curcumin relative to non-cross-linked HA (Fig. 5). In contrast, no appreciable reduction in diffusion was observed for gardenia blue or FD&C Blue No. 1.

These results suggest that hydrogel cross-linking selectively influences the mobility of hydrophobic dyes, likely by restricting molecular transport within the swollen polymer network. Water-soluble dyes, however, readily migrate through the hydrated cHA matrix and into surrounding tissue, rendering cross-linking ineffective in limiting their diffusion. The observed behavior underscores the dominant role of dye solubility in governing intradermal transport, even in the presence of a structurally constrained matrix.

4. Conclusions

This study demonstrates the feasibility of a detachable HA microneedle platform as a materials-based approach for intradermal placement of tattoo colorants and for systematically evaluating their diffusion and retention behavior in skin. A diverse set of colorants, including conventional synthetic tattoo pigments, FD&C dyes, natural pigments, and natural dyes, was successfully incorporated into HA microneedles without compromising structural integrity or transfer reliability. Clear distinctions were observed between pigment-type and dye-type colorants. Insoluble pigments generated vivid and spatially stable patterns with minimal diffusion, whereas molecular dyes exhibited rapid spreading and reduced pattern persistence. Pigment particle size was identified as a critical factor governing both microneedle fabrication and intradermal retention, with intermediate-sized particles (3–5 μm) providing the most favorable balance between color intensity and stability. Modification of the microneedle matrix through HA cross-linking selectively reduced the diffusion of hydrophobic dyes but had little effect on water-soluble dyes, underscoring the dominant role of colorant solubility in governing intradermal transport.

Overall, these findings highlight how colorant chemistry, particle size, and matrix structure collectively dictate diffusion behavior and pattern stability in microneedle-assisted tattoo systems. The results provide materials-level insight into the rational design of alternative tattoo colorants and delivery platforms and offer a comparative framework for selecting pigments and dyes based on their physicochemical properties.

Declarations

Author contributions

Kornkamol Obthong: writing original draft, review manuscript, analysis, investigation, methodology, project administration; **Supanan Ampawa:** analysis, preliminary investigation, review

manuscript; **Supason Wanichwecharungruang:** supervision, conceptualization, writing original draft, finalizing manuscript, funding acquisition

Funding Declaration

His Royal Highness Crown Prince Maha Vajiralongkorn Scholarship for K.O., from the Graduate School, Chulalongkorn University, is gratefully acknowledged. The authors also thank the Center of Excellence in Advanced Materials and Bio-Interfaces at Chulalongkorn University, and Mineed Technology, for financial support.

Clinical trial number

Not applicable.

Conflict of interest statement

Mineed Technology Co., Ltd. owns intellectual property related to the detachable microneedle platform used in this work, and one author is affiliated with the company. The study was conducted as an academic materials investigation. The remaining authors declare no competing interests.

Consent to Publish

Not applicable.

Ethics approval and consent to participate

Since this study utilized porcine tissue obtained from a commercial food production slaughterhouse, it did not involve live animal experimentation and did not require formal ethical approval. Informed consent is not applicable as no human subjects were involved

Data availability statement

The data that support the findings of this study are available from the corresponding author upon reasonable request.

References

1. Chalarca-Cañas D, Caviedes-Cleves MA, Correa-Londoño LA, Ospina-Gómez JP, Velásquez-Lopera MM. Tattoos: risks and complications, clinical and histopathological approach. Bras Dermatol. 2024;99:491–502. https://doi.org/10.1016/j.abd.2023.07.004.
2. Kerure AS, Marwah M, Wagh ND, Udare S, Micropigmentation. Indian Dermatol Online J. 2023;14:605–10. https://doi.org/10.4103/idoj.idoj_767_21.
3. Townend C, Landeg S, Thorne R, Kirby AM, McNair HA. A review of permanent marking for radiotherapy in the UK. Radiography (Lond). 2020;26:9–14.

https://doi.org/10.1016/j.radi.2019.08.003.

4. Giulbudagian M, Schreiver I, Singh AV, Laux P, Luch A. Safety of tattoos and permanent make-up: a regulatory view. Arch Toxicol. 2020;94:357–69. https://doi.org/10.1007/s00204-020-02655-z.
5. Schubert S, Kluger N, Schreiver I. Hypersensitivity to permanent tattoos: Literature summary and comprehensive review of patch tested tattoo patients 1997–2022. Contact Dermat. 2023;88:331–50. https://doi.org/10.1111/cod.14291.
6. Li S, Kim Y, Lee JW, Prausnitz MR. Microneedle patch tattoos. iScience. 2022;25:105014. https://doi.org/10.1016/j.isci.2022.105014.
7. Fraser TR, Ross KE, Alexander U, Lenehan CE. Current knowledge of the degradation products of tattoo pigments by sunlight, laser irradiation and metabolism: a systematic review. J Expo Sci Environ Epidemiol. 2022;32:343–55. https://doi.org/10.1038/s41370-021-00364-y.
8. Forbat E, Al-Niaimi F. Patterns of reactions to red pigment tattoo and treatment methods. Dermatol Ther (Heidelb). 2016;6:13–23. https://doi.org/10.1007/s13555-016-0104-y.
9. Bose R, Sibley C, Fahim S. Granulomatous and systemic inflammatory reactions from tattoo ink: Case report and concise review. SAGE Open Med Case Rep. 2020;8:2050313X20936036. https://doi.org/10.1177/2050313X20936036.
10. Bäumler W. Chemical hazard of tattoo colorants. Presse Med. 2020;49:104046. https://doi.org/10.1016/j.lpm.2020.104046.
11. Dodig S, Čepelak-Dodig D, Gretić D, Čepelak I. Tattooing: immediate and long-term adverse reactions and complications. Arh Hig Rada Toksikol. 2024;75:219–27. https://doi.org/10.2478/aiht-2024-75-3921.
12. Baranska A, Shawket A, Jouve M, Baratin M, Malosse C, Voluzan O, et al. Unveiling skin macrophage dynamics explains both tattoo persistence and strenuous removal. J Exp Med. 2018;215:1115–33. https://doi.org/10.1084/jem.20171608.
13. Schreiver I, Hesse B, Seim C, Castillo-Michel H, Villanova J, Laux P, et al. Synchrotron-based v-XRF mapping and μ-FTIR microscopy enable to look into the fate and effects of tattoo pigments in human skin. Sci Rep. 2017;7:11395. https://doi.org/10.1038/s41598-017-11721-z.
14. Serup J. Chaotic tattoo ink market and no improved costumer safety after new EU regulation. Dermatology. 2023;239:1–4. https://doi.org/10.1159/000526338.
15. Koo H. Effectiveness of dyes as skin biopsy markers. MSc thesis. North Carolina State University; 2018.
16. Atwater AR, Bembry R, Reeder M. Tattoo hypersensitivity reactions: inky business. Cutis. 2020;106:64–7. https://doi.org/10.12788/cutis.0028.
17. Shammout MA, Alsaleh MM, Natsheh IY, Albadawi DK, Alkhawaldeh AK. Dyes are the rainbow of our health. Chem (Basal). 2023;5:2229–45. https://doi.org/10.3390/chemistry5040149.
18. Toprangkobsin P, Teepakakorn A, Ampawa S, Efendi A, Limcharoen B, Banlunara W, et al. Detachable microneedles with crosslinked hyaluronic acid as superficial skin filler. J Biomed Mater Res A.

2025;113:e37933. https://doi.org/10.1002/jbm.a.37933.

19. Yin M, Zeng Y, Liu HQ, Zhang W, Wang C, Chen C, et al. Dissolving microneedle patch integrated with microspheres for long-acting hair regrowth therapy. ACS Appl Mater Interfaces. 2023;15:17532–42. https://doi.org/10.1021/acsami.2c22814.
20. Fakhraei Lahiji S, Kim Y, Kang G, Kim S, Lee S, Jung H. Tissue interlocking dissolving microneedles for accurate and efficient transdermal delivery of biomolecules. Sci Rep. 2019;9:7886. https://doi.org/10.1038/s41598-019-44418-6.
21. Oh H, Lee JS, Son P, Ryu H, Kim OB, Choi WI. Highly stable and safe biocompatible black tattoo ink based on Pluronic polymer-coated carbon black nanoparticles. Dyes Pigm. 2025;235:112627. https://doi.org/10.1016/j.dyepig.2024.112627.

Figures

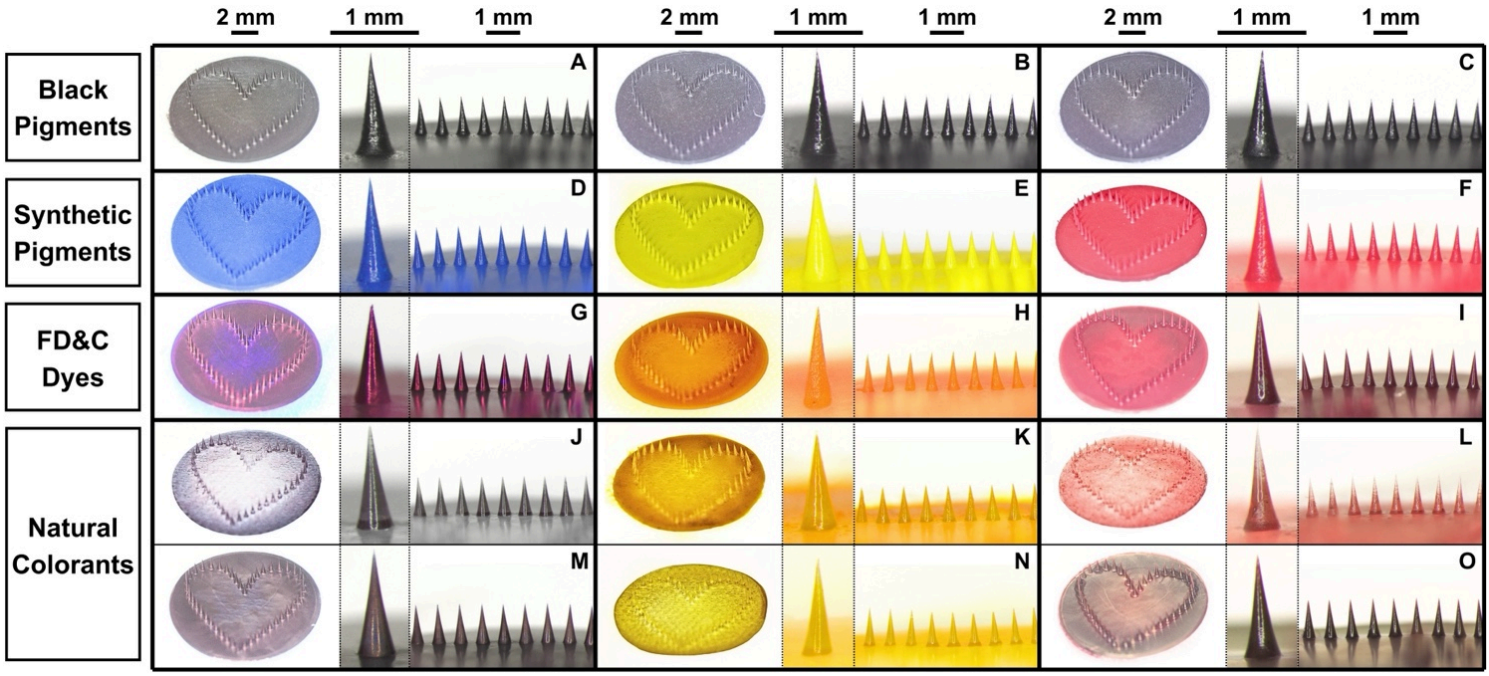


Figure 1

Morphology of tattoo microneedle patches loaded with different colorants. Each rectangular panel presents three stereomicroscopic views of a single tattoo microneedle patch: the whole patch (left) and side-view images of the microneedles at two magnifications (middle and right). Scale bars corresponding to each magnification are shown at the top of each column. The microneedles are loaded with carbon black (A), bamboo charcoal (B), melanin black (C), blue tattoo pigment (D), yellow tattoo pigment (E), red tattoo pigment (F), FD&C Blue No. 1 (G), FD&C Yellow No. 5 (H), FD&C Red No. 40 (I), butterfly pea (J), curcumin (K), beetroot (L), gardenia blue (M), beta-carotene (N), and red yeast rice (O).

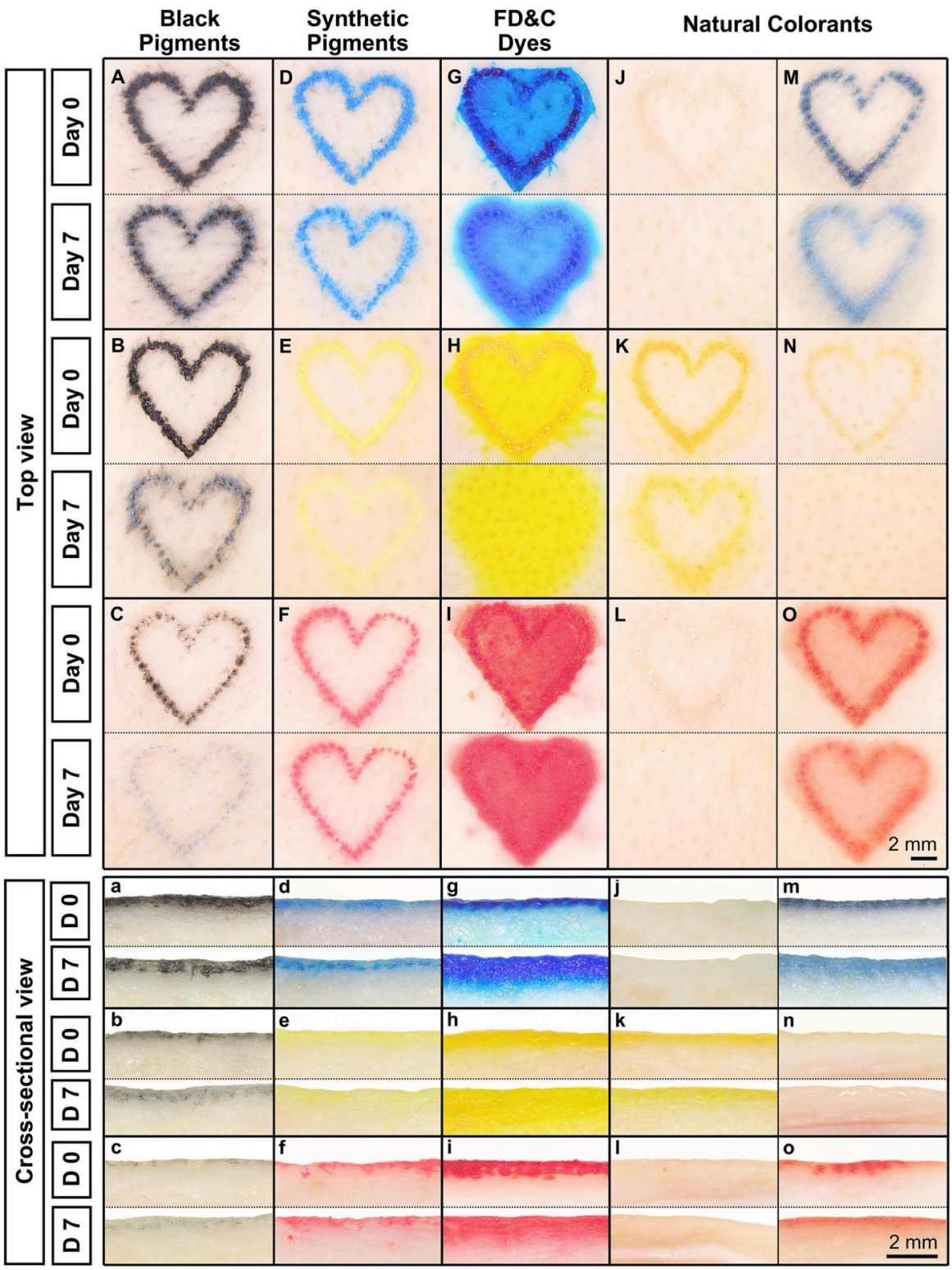


Figure 2

Tattoo pattern transfer and retention on *ex vivo* porcine skin. Stereomicroscopic images of tattoo patterns on porcine skin surfaces (A–O) and corresponding cross-sectional images of the skin (a–o). Surface images were captured immediately after application (top) and at 7 days post-application (bottom). Cross-sectional images were obtained immediately after application (top) and at 7 days post-application (bottom). The colorants used were carbon black (A, a), bamboo charcoal (B, b), melanin

black (C, c), blue tattoo pigment (D, d), yellow tattoo pigment (E, e), red tattoo pigment (F, f), FD&C Blue No. 1 (G, g), FD&C Yellow No. 5 (H, h), FD&C Red No. 40 (I, i), butterfly pea (J, j), curcumin (K, k), beetroot (L, l), gardenia blue (M, m), beta-carotene (N, n), and red yeast rice (O, o).

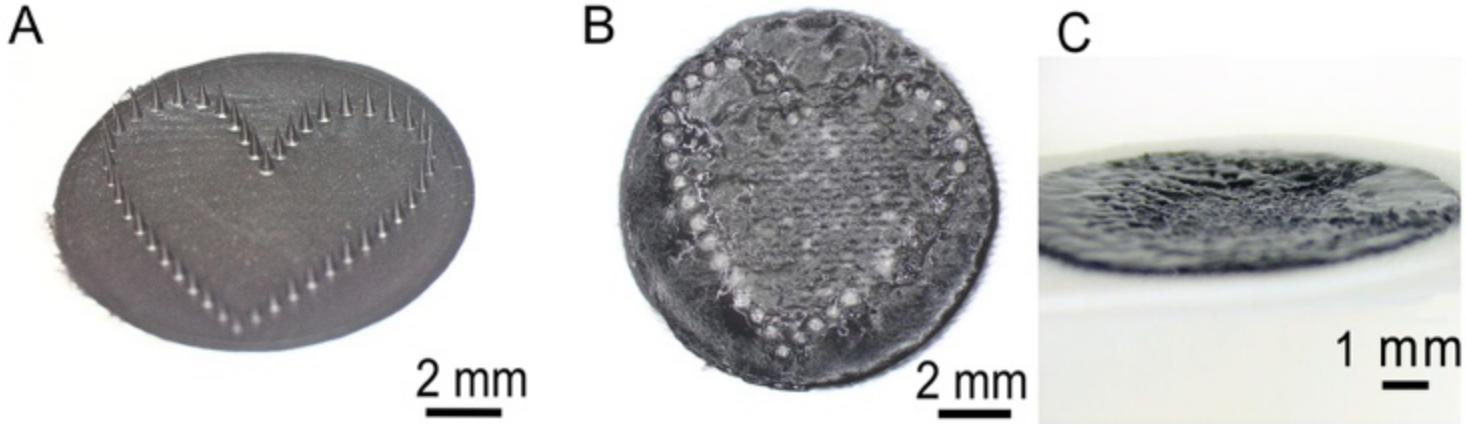


Figure 3

Patch backing before and after application. Stereomicroscopic images of a tattoo microneedle patch before application (A) and after removal from the skin (B and C), showing complete detachment of the microneedles from the backing layer.

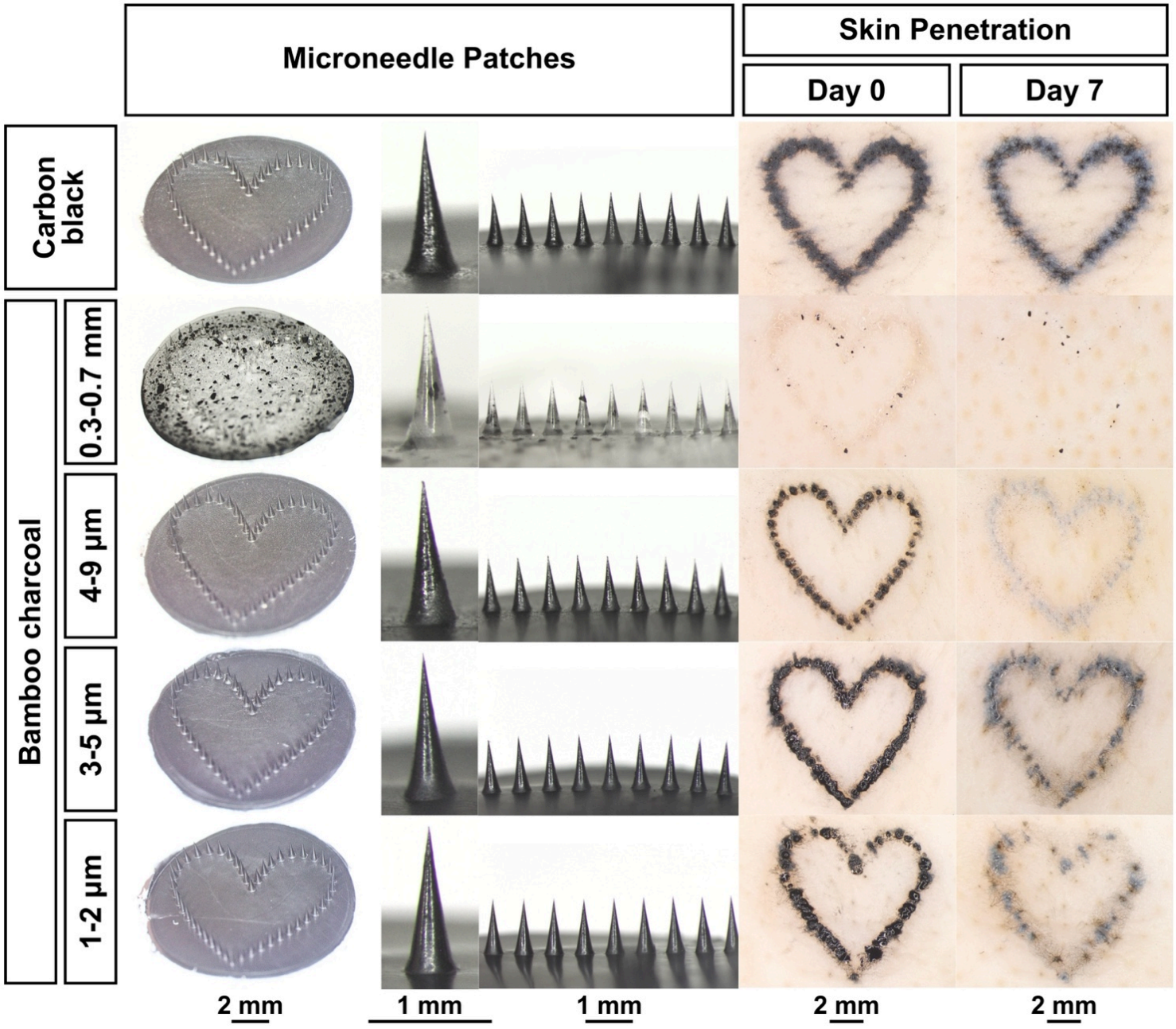


Figure 4

Effect of pigment particle size on microneedle fabrication and tattoo pattern stability. Stereomicroscopic images of microneedle patches loaded with carbon black (top row) and bamboo charcoal of different particle sizes: 0.3–0.7 mm (second row), 4–9 µm (third row), 3–5 µm (fourth row), and 1–2 µm (bottom row). For each formulation, corresponding stereomicroscopic images of *ex vivo* porcine skin surfaces at Day 0 and Day 7 post-application are shown on the right.

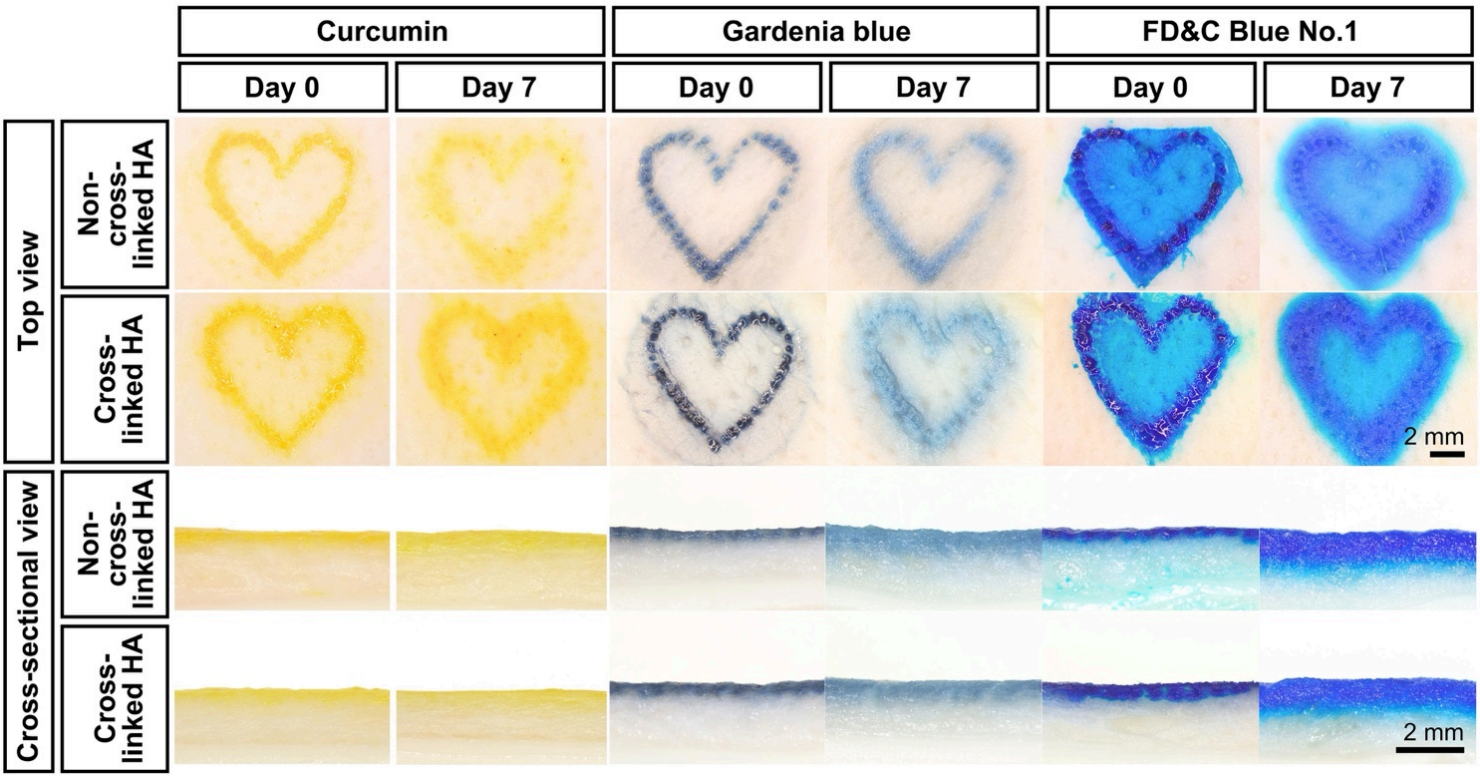


Figure 5

Influence of HA cross-linking on colorant diffusion in porcine skin. Top-view stereomicroscopic images (top panels) and corresponding cross-sectional images (bottom panels) of *ex vivo* porcine skin after application of microneedle patches fabricated from non-cross-linked HA and cross-linked HA. Microneedles were loaded with curcumin, gardenia blue, and FD&C Blue No. 1 (left to right). Skin images were obtained immediately after application and at 7 days post-application to evaluate the effect of matrix cross-linking on colorant diffusion.

Supplementary Files

This is a list of supplementary files associated with this preprint. Click to download.

- SupplementaryInformation.docx
- image1.jpeg